

Abnormal characterization of dynamic functional connectivity in Alzheimer's disease

<https://doi.org/10.4103/1673-5374.332161>

Date of submission: April 6, 2021

Date of decision: June 10, 2021

Date of acceptance: November 12, 2021

Date of web publication: February 8, 2022

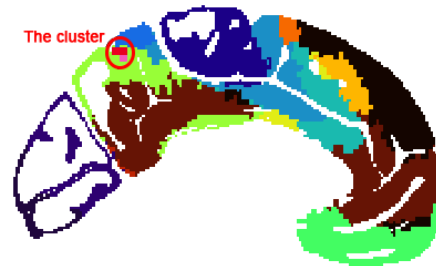
From the Contents

Introduction	2014
Participants and Methods	2015
Results	2017
Discussion	2019

Cui Zhao^{1,2,#}, Wei-Jie Huang^{3,4,5,#}, Feng Feng^{6,7}, Bo Zhou¹, Hong-Xiang Yao⁸, Yan-E Guo¹, Pan Wang⁹, Lu-Ning Wang¹, Ni Shu^{3,4,5,*}, Xi Zhang^{1,*}

Graphical Abstract

Differences in the strength of dynamic functional connectivity among individuals with amnesic mild cognitive impairment, Alzheimer's disease, and normal controls



Abstract

Numerous studies have shown abnormal brain functional connectivity in individuals with Alzheimer's disease (AD) or amnesic mild cognitive impairment (aMCI). However, most studies examined traditional resting state functional connections, ignoring the instantaneous connection mode of the whole brain. In this case-control study, we used a new method called dynamic functional connectivity (DFC) to look for abnormalities in patients with AD and aMCI. We calculated dynamic functional connectivity strength from functional magnetic resonance imaging data for each participant, and then used a support vector machine to classify AD patients and normal controls. Finally, we highlighted brain regions and brain networks that made the largest contributions to the classification. We found differences in dynamic function connectivity strength in the left precuneus, default mode network, and dorsal attention network among normal controls, aMCI patients, and AD patients. These abnormalities are potential imaging markers for the early diagnosis of AD.

Key Words: Alzheimer's disease; amnesic mild cognitive impairment; blood oxygen level-dependent; default mode network; dynamic functional connectivity; frontoparietal network; resting-state functional magnetic resonance imaging; support vector machine

Introduction

A patient is diagnosed with dementia every 3 seconds, and the global number of people with dementia is expected to reach more than 70 million by 2030 (McDade and Bateman, 2017). Alzheimer's disease (AD) is one of the most common causes of dementia in older adults. Despite the tremendous burden for patients, their families, and societies, effective treatments for AD are still lacking (Tiwari et al., 2019). Amnesic mild cognitive impairment (aMCI) has been regarded as a transitional stage between normal aging and AD (Blennow and Hampel, 2003). Interestingly, not all aMCI patients experience further progression. Thus, studying aMCI and AD patients simultaneously might aid the discovery of biomarkers of disease progression (Drago et al., 2011). Making timely and effective diagnoses in the early stages of AD could lead to promising opportunities for interventions (Grady et al., 1988; Jack et al., 2010).

Functional magnetic resonance imaging (fMRI) is used to noninvasively obtain brain activity information by measuring blood oxygen level-dependent signals (Logothetis and Wandell, 2004; Cai et al., 2020; Huang et al., 2020; Xing et al., 2021). Previous fMRI and structural MRI studies have shown evidence of reduced gray matter volume and cortical thickness in multiple brain regions (Wenk, 2003; Suzuki et al., 2019) in the preclinical phase of AD, and these changes are strongly associated with altered cognitive function. In particular, resting-state fMRI has great potential for discovering biomarkers of AD, which could facilitate early diagnosis of AD and understanding of the underpinning mechanisms (Luo et al., 2019). Widespread alterations in connectivity among multiple brain systems have been reported in AD patients (Dennis and Thompson, 2014). For instance, AD patients exhibited decreased connectivity in the default mode network (DMN), as well as altered functional connectivity between the default-mode and salience network (Schultz et al., 2017).

¹Department of Neurology, Second Medical Center, National Clinical Research Center for Geriatric Disease, Chinese PLA General Hospital, Beijing, China;

²Department of Geriatrics, Affiliated Hospital of Chengde Medical University, Chengde, Hebei Province, China; ³State Key Laboratory of Cognitive Neuroscience and Learning, Beijing Normal University, Beijing, China; ⁴Center for Collaboration and Innovation in Brain and Learning Sciences, Beijing Normal University, Beijing, China; ⁵Beijing Key Laboratory of Brain Imaging and Connectomics, Beijing Normal University, Beijing, China; ⁶Department of Neurology, First Medical Center, Chinese PLA General Hospital, Beijing, China; ⁷Department of Neurology, PLA Rocket Force Characteristic Medical Center, Beijing, China; ⁸Department of Radiology, Second Medical Center, Chinese PLA General Hospital, Beijing, China; ⁹Department of Neurology, Tianjin Huanhu Hospital, Tianjin, China

*Correspondence to: Ni Shu, PhD, nshu@bnu.edu.cn; Xi Zhang, MD, smrc301@163.com.

<https://orcid.org/0000-0002-4598-714X> (Xi Zhang)

#Both authors contributed equally to this work.

Funding: This study was supported by the National Natural Science Foundation of China, No. 81471120; and Fund Projects in Technology of the Foundation Strengthening Program of China, No. 2019-JC1Q-JJ-151 (both to XZ).

How to cite this article: Zhao C, Huang WJ, Feng F, Zhou B, Yao HX, Guo YE, Wang P, Wang LN, Shu N, Zhang X (2022) Abnormal characterization of dynamic functional connectivity in Alzheimer's disease. *Neural Regen Res* 17(9):2014-2021.

These large-scale dynamic network abnormalities were related to reduced cognitive performance, as well as to the levels of molecular biomarkers of AD and AD-related genetic risk factors (Wang et al., 2021).

Static resting-state functional connectivity has been widely used to measure the correlation between averaged time courses in different brain regions. However, dynamic connectivity analysis is used to calculate the variability of functional connectivity over time by considering temporal fluctuations within varying windows (Hutchison et al., 2013). Dynamic functional connectivity (dFC) has certain advantages with respect to static connectivity, such as providing more useful information to distinguish patients from healthy controls (Rashid et al., 2014). One of these novel measures is dFC strength (dFCS), which represents the strength of the dynamic correlation between the time series of voxels. This measure reflects the dynamic interconnections between brain regions from the voxel perspective (Luo et al., 2019). However, few studies have investigated the variability of dFCS in AD patients, especially in the aforementioned DMN. Based on a series of previous studies, we hypothesized that, compared with cognitively normal older adults, the dFCs of the DMN would be low in patients with AD and aMCI, and that this would be associated with overall cognitive ability.

dFC features can reflect detailed changes in brain activity (Du et al., 2017). When static and dFC features were compared in terms of utility in clinical disease recognition, the dFC features were more accurate in identifying diseases, and combining static and dynamic features did not lead to a significant improvement in accuracy (Rashid et al., 2016). Numerous studies have indicated that dFC is better able to distinguish patients from controls compared with state functional connection analysis (Rashid et al., 2014; Chen et al., 2018; Yang et al., 2019), which is widely used in studies of autism (Chen et al., 2017), schizophrenia (Duan et al., 2020), and depression (Liao et al., 2018). In recent years, some investigators have used the dynamic amplitude of low frequency fluctuation signals to examine characteristics of AD (Zeng et al., 2019), but few studies have compared dFC among AD, aMCI, and normal control (NC) groups.

Rapid developments in computer science and the accumulation of brain imaging data have provided clinical researchers with new approaches for differentiating and predicting AD and aMCI (Pereira et al., 2009). One of these techniques is a machine learning algorithm called a support vector machine (SVM). SVMs map the input vectors (input data) into a high-dimensional feature space and then compute a hyperplane that divides these input vectors into two classes. SVMs have been extensively used in AD pathology research, drug development, and computer-aided diagnoses (Haller et al., 2011). For instance, Zhao et al. (2019) used a SVM to identify 257 microRNAs associated with AD. Lv and Xue (2010) improved the effectiveness of a SVM in predicting inhibitors of acetylcholinesterase, a drug for AD, using a new feature selection method. Chaves et al. (2009) obtained a diagnostic accuracy of 98.3% for early AD diagnosis using voxels in the temporal and parietal regions as features. Recently, resting-state fMRI data has become much easier to collect, making it a useful tool for discovering the biomarkers of AD. Furthermore, dynamic connectivity (e.g. dFCS) can provide more information about how neural processes change over time (Ma et al., 2020). However, no studies have employed SVMs to conduct aMCI-NC and AD-NC classifications using dFCS variability as features.

To examine our above-mentioned hypothesis, we compared differences in dFCS at the voxel level among three groups (AD, aMCI, and NC), and then explored the relationship between comprehensive cognitive performance and dFCS variability in statistically significant regions. In addition, to investigate potential dFCS variability in pre-clinical diagnoses of AD, we trained two SVM models to conduct aMCI-NC and AD-NC classifications, respectively, and visualized the weights of brain regions and brain networks that contributed to the classification.

Participants and Methods

Participants

This case-control study was approved by the Institutional Ethics Committee of the General Hospital of the Chinese PLA General Hospital (approval No. 20100317-001) on April 28, 2010 (Additional file 1). All subjects were recruited from the Neurology Outpatient Clinic of PLA General Hospital (Beijing, China) between January 1, 2017 and March 12, 2020, and two experts (BZ and YEG) were involved in the final diagnosis of each subject. All subjects agreed to

participate and signed ethical informed consent forms (Additional file 2). They underwent standard pre-experimental physical and psychological examination batteries, neuropsychological screening, and a cranial magnetic resonance scan. A total of 107 subjects were included in this study, including 36 patients with AD, 30 patients with aMCI, and 41 individuals who were cognitively NC. This study was conducted in accordance with the Strengthening the Reporting of Observational Studies in Epidemiology (STROBE) statement (von Elm et al., 2007) (Additional file 3).

Selection criteria

We included AD patients who (1) met the criteria for AD diagnosis jointly developed by the National Institute of Neurological and Communicative Disorders and Stroke (NINCDS) (McKhann et al., 1984) and the Alzheimer’s Diseases and Related Disorders Association (ADDA) (McKhann et al., 1984); (2) had a final score of 1 or 2 on the Clinical Dementia Rating Scale (CDR) (Sperling et al., 2011); (3) had no history of use of medications that affect cognition (e.g., acetylcholinesterase inhibitors, NMDA receptor antagonists); and (4) were aged 60–80 years.

In accordance with Peterson’s criteria (Peterson et al., 2014) for mild cognitive impairment, we selected aMCI patients with (1) self-reported cognitive decline or confirmed decline from a knowledgeable person, with clinically significant symptoms of cognitive decline that had persisted for at least six months, and who did not meet the criteria for a dementia diagnosis; (2) a score of 0.5 on the CDR; (3) an activities of daily living score (Peterson et al., 2001) of 26 or less and no significant impairment in the ability to perform activities of daily living; and (4) a Mini-Mental State Examination (MMSE) score (Peterson, 2004) no less than 24. We selected normal controls who were over 65 years old with a CDR score of 0, activities of daily living score less than 26, and MMSE score greater than 24.

We excluded patients with a Hachinski ischemic index score (Pantoni and Inzitari, 1993) of 4 or more, hypothyroidism, vitamin B12 or folic acid deficiency, a long history (more than 5 years) of smoking and alcohol abuse, inability to complete an MRI scan (patients with contraindications to MRI scanning, i.e., severely febrile, critically ill, claustrophobic, in early pregnancy, and with metal implants in the body or metal foreign bodies) or neuropsychological testing, traumatic brain disease or a history of other brain disorders, Parkinson’s syndrome, epilepsy, and those with other systemic neurological disorders that severely affect cognitive function and systemic disorders that can affect MRI scans or neuropsychological tests. We excluded patients whose fMRI images failed visual quality control or pre-processing. The trial procedure is shown in Figure 1.

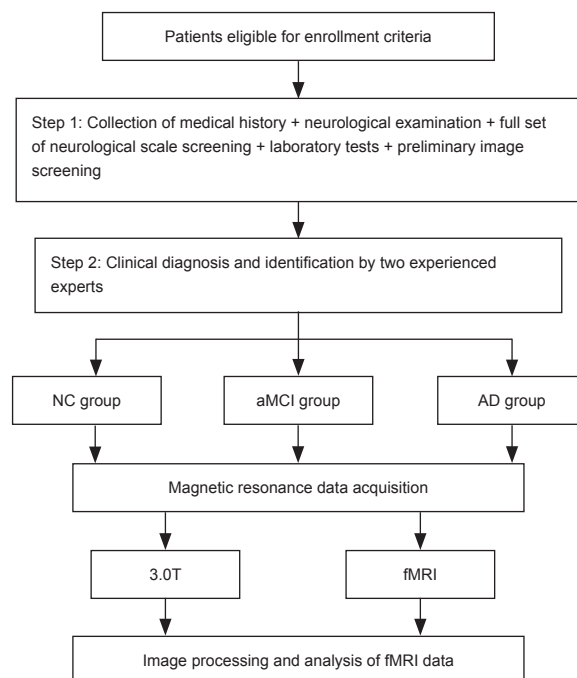


Figure 1 | Patient flow chart.

AD: Alzheimer’s disease; aMCI: amnesic mild cognitive impairment; fMRI: functional magnetic resonance imaging; NC: normal control.

Neuropsychological tests

All subjects underwent a series of neuropsychological tests, including the MMSE, CDR, Geriatric Depression Scale (GDS), Montreal cognitive assessment (MoCA), and the Activities of Daily Living Scale (ADLS). The MMSE is currently the most widely used scale for evaluating cognitive function. It is simple and easy to implement, and includes items about time, place, calculation, and memory. The total score ranges from 0–30 points, and lower scores reflect worse cognitive function (Petersen, 2004). The MoCA is used to quickly screen for mild cognitive dysfunction. It includes a total of eight tests measuring different cognitive domains such as memory, executive function, visual space, and attention. The maximum score is 30 points. If the patient has 12 or fewer years of education, 1 point is added to the total score. A lower score reflects worse cognitive function. The CDR is mostly used to assess the degree of cognitive impairment in patient populations, and covers memory, orientation, judgment, problem-solving, and social activities. The total score is expressed as 0, 0.5, 1, 2, or 3 points. A higher score reflects worse cognitive function (Sperling et al., 2011). We also used the GDS-15, which is currently recommended by the American Academy of Geriatrics for screening depression in older people, and has a total score of 0–15. Higher scores represent more serious depression. Patients with > 4 points on the GDS-15 were excluded from this study. Finally, we used the ADLS, which includes the basic ADL and instrumental ADL, and covers 20 activities such as eating, dressing, bathing, and handling money independently. The ADL is considered to be the most appropriate assessment of activity ability in elderly individuals. Each item is worth 1–9 points, for a total of 20–180 points. A higher score indicates worse living ability.

fMRI

Image acquisition and preprocessing

MRI images were acquired by an experienced physician using a Siemens 3.0T MRI scanner with a 20-channel cranial coil. Scanning was conducted at the outpatient clinic of the Department of Radiology, Chinese PLA General Hospital. fMRI images were acquired using a gradient echo combined with a single excitation echo planar imaging sequence (64 × 64 resolution, 2000 ms repetition time, 30 ms echo time, 30 axial layers with 1 mm layer space and 3 mm thickness, 220 mm × 220 mm field of view, 90 flip angle, and duration of 8 minutes 6 seconds). We used the following protocol to obtain better MRI quality. First, all subjects underwent safety training prior to image acquisition. The subjects wore latex earplugs and a fixed head strap throughout the scan to minimize the effects of instrument noise and involuntary head movements. They were asked to lie down and relax with their eyes closed, and to avoid systematic thinking during the scan.

We used DPASFA (Data Processing Assistant for Resting-State fMRI package, version 4.2; <http://www.restfmri.net>) for fMRI preprocessing. Briefly, the standard process is as follows. First, we excluded the first 10 volumes in each fMRI dataset to account for changes in the magnetic field stability during scanning and the subject's adaptability to the scanning environment. Second, we corrected the data for participant head movements and slice-timing (Buchanan et al., 2020). Third, we registered all images to standard Montreal Neurological Institute neuroimaging space and performed spatial correction with a full width at half maximum Gaussian kernel function to reduce individual anatomical structure differences and spatial noise (resample resolution of 3 mm × 3 mm × 3 mm and kernel length-width-height of 6 mm × 6 mm × 6 mm). Finally, we denoised the data via linear regression and a subsequent temporal band-pass filter (0.01–0.1 Hz) to regress out interfering covariates including Friston 24 motion parameters, linear drift, white matter signal, and cerebrospinal fluid signal.

dFCS

We used the DynamicBC toolkit (v1.1, www.restfmri.net/forum/DynamicBC) to calculate the global dFCS for each voxel with the sliding window approach, as shown in the flow chart in **Figure 2**. We set the length of the window to 50 repetitions with an overlap of 0.6. The rest of the parameters were identical to a previous study (Luo et al., 2019) (230 total repetitions were available and 7 windows were created.) For each window, we first calculated the global dFCS at each voxel as the sum of the functional connectivity between this voxel and the other voxels in the brain mask. We adopted the threshold $P < 0.001$ to eliminate voxels with weak correlations attributable to signal noise and removed negative correlations. Then, we obtained a series of dFCS maps corresponding to the number of windows. The variance of each dFCS map across time was calculated to measure

its temporal variability. Finally, on the basis of a previous study, the variance of the dFCS map for each subject was transformed to a Z score by subtracting the mean values divided by the standard deviation of all values within the brain mask to control the global effects (Zou et al., 2008).

Data analysis

Data analysis was performed using the DynamicBC toolbox in Matlab 2018b (The MathWorks, Inc., Natick, MD, USA) as described below. First, we compared demographic factors, including age, gender, and years of education using either an analysis of variance or the Chi-squared test among the AD, aMCI, and NC groups. Second, we conducted a voxel-wise one-way analysis of covariance with age, gender, and education as covariates to determine the altered variance of dFCS among the three groups. We corrected the results via threshold-free cluster enhancement correction (Smith and Nichols, 2009) at a significance level of 0.05. Third, we extracted the variance of the dFCS values with significant differences among the three groups by summing the Z scores of the clusters with statistical significance, and then conducted between-group comparisons via two-tailed two-sample t-tests. Finally, to investigate the relationship between cognitive ability and dFCS variability in statistically significant regions, we conducted a partial correlation analysis of dFCS variance with MMSE scores and MoCA, controlling for age, gender, and years of education.

To discriminate aMCI and AD from NC, we used the variance of dFCS maps as features and trained linear SVM models using LIBSVM 3.25 (<https://www.npckd.org/p/libsvm/3.25>). This led to a model with more interpretability than other non-linear models and less susceptibility to over-fitting. Because of the limited study population, we used 5-fold cross validation (**Figure 3**) to evaluate the performance of the models. In each model, four-fifths of the participants were selected as the training dataset, and the other participants were used as the test dataset. Because the classification was pair-wise, we used a two-sample t-test to select the features with P values < 0.05 in the training dataset. Although they can preserve multivariate patterns, we did not use multivariate feature selection methods such as recursive feature elimination because they are time-consuming. Before inputting the data into the model, we normalized the features using the mean values and standard deviations from the training dataset. We used the accuracy, sensitivity, specificity, area under the curve, positive predictive value, negative predictive value, and F-score to evaluate model performance. We used the permutation test to determine whether the obtained final metrics were significantly better than chance. Specifically, we ran the above prediction procedure 1000 times. For each time, we permuted the labels across the samples without replacements. The P values of the metrics were calculated by dividing the number of permutations with a higher value than the actual value for the real sample by the total number of permutations. For each sample, we also calculated the decision value, which is the distance between the samples on a hyperplane that is determined by SVM classifiers. We also used partial correlation analysis to explore the relationship between decision values and MMSE and MoCA scores.

Finally, we visualized the distribution of voxels contributing to the classifier by summing the weights (absolute weight)/distributions of the voxels separately on the brain region or network level using LIBSVM 3.25. Ninety brain regions were defined using the AAL template in standard space (Tzourio-Mazoyer et al., 2002). The whole brain was divided into seven networks based on a functional partition, as described by Yeo et al. (2011): visual network, somatomotor network, dorsal attention network, ventral attention network, limbic network, frontoparietal network, and DMN. The specific coordinates and detailed functions of the brain regions in these seven networks can be found in Bargmann and Marder (2013). We also conducted a follow-up analysis. The goal of the training process for the SVM model was to determine a hyperplane and separate the different types of samples in the feature space. The coefficients defined by the hyperplane can be used to quantify the contribution of different features in the classification task, that is, the greater the absolute value of the coefficients, the greater the contribution of the corresponding features. We coded the patient sample as 1 and the control group as -1. Compared with the controls, the patient group had a higher number of features with positive coefficients in the hyperplane, that is, with positive contributions. In contrast, the eigenvalues with negative coefficients, that is, those with negative contributions, tended to be lower in the patient group. The statistical methods of this study were reviewed by the biostatistician of Chinese PLA General Hospital.

Results

Demographic features of AD, aMCI, and NC groups

We found no significant differences in age, gender ratio, or years of education among the three groups ($P > 0.05$). However, the MMSE and MoCA scores were significantly different ($P < 0.001$), with the lowest scores for AD patients, highest scores for NCs, and intermediate scores for aMCI patients (Table 1).

Table 1 | Demographic and neuropsychological data for the AD, aMCI and NC groups

Item	AD (n=36)	aMCI (n=30)	NC (n=41)	F-value	P-value
Age (yr)	71.6±8.8	69.4±8.8	68.3±6.8	3.0491	0.2177
Sex (male/female)	16/20	11/19	21/20	0.0376	0.9814
Education (yr)	9.7±4.5	12.1±4.0	12.1±4.3	0.4472	0.7996
MMSE score	17.72±6.0	26.83±2.13	28.51±1.36	86.6850	< 0.001
MoCA score	14.37±3.15	22.11±2.62	26.64±2.65	104.5989	< 0.001

Data are expressed as mean ± SD, and were analyzed by one-way analysis of variance, except sex with number and analyzed by Chi-squared test. AD: Alzheimer’s disease; aMCI: Amnesic mild cognitive impairment; MMSE: Mini-mental state examination; MoCA: Montreal Cognitive Assessment; NC: Normal control.

Significant differences in the left precuneus among the AD, aMCI, and NC groups

Using voxel-wise analysis, we found significant differences in dFCS variance in a cluster including the left precuneus among the three groups (Figure 4A). The Montreal Neurological Institute coordinates of the peak voxel, which had an F value of 12.03, were (−3, −60, 57) and the cluster size was 6. Then, we extracted the mean variance of the dFCS in the left precuneus. A two-tailed two-sample t-test (Figure 4B) showed that the mean variances of the dFCS in the left precuneus region of patients with aMCI ($P < 0.01$) and AD ($P < 0.001$) were lower than that in the NC group.

dFCS variance in the left precuneus was positively correlated with MMSE and MoCA scores

A partial correlation analysis controlling for sex, age, and education revealed that the mean variance of the dFCS in the left precuneus was significantly positively correlated with MMSE ($r = 0.29, P = 0.003$) and MoCA ($r = 0.24, P = 0.038$) scores (Figure 5).

Performance of classifiers

As shown in Table 2, except for the specificity and positive predictive value, for which the aMCI-NC classifier was better than the AD-NC classifier, the aMCI-NC classifier did not perform as well as the AD-NC classifier in all other measured domains.

Table 2 | Performance of classifying the AD and aMCI groups from the NC group

	NC vs. aMCI		NC vs. AD	
	Data	P-value	Data	P-value
Accuracy	0.68	0.007	0.71	0.004
Sensitivity	0.40	0.009	0.72	0.001
Specificity	0.88	0.031	0.71	0.039
Area under curve	0.61	0.05	0.75	0.001
Positive predictive value	0.71	0.014	0.68	0.031
Negative predictive value	0.67	0.006	0.74	0.003
F-score	0.51	0.011	0.7	0.001

AD: Alzheimer’s disease; aMCI: amnesic mild cognitive impairment; NC: normal control.

We performed a partial correlation analysis to explore whether the decision values generated from the SVM classifiers were correlated with the MMSE and MoCA scores. As shown in Figure 6, the decision values were significantly correlated with the MMSE ($r = 0.42, P < 0.001$) and MoCA ($r = 0.27, P = 0.016$) scores.

Brain regions that most strongly contributed to classification

To identify the brain regions that most strongly contributed to

classification, we calculated the mean positive and negative weights, respectively, for each region. Table 3 shows the ten regions that most negatively and positively contributed to the classification of aMCI and NC. Most of the contributive regions were in the frontal and temporal lobes, while some regions in the frontal, temporal, and occipital regions positively contributed to classification.

Table 3 | The ten regions that contributed most to the classification of the aMCI from the NC group

Region	Absolute weight ($\times 10^{-5}$)
Negatively	
Left superior temporal gyrus	3.94
Left parahippocampal gyrus	3.84
Left rolandic sulcus	3.59
Right parahippocampal gyrus	3.06
Right Heschl’s gyrus	2.93
Right middle orbitofrontal cortex	2.37
Left superior orbitofrontal cortex	2.36
Right superior frontal gyrus	2.32
Left Heschl’s gyrus	2.32
Left amygdala	2.31
Positively	
Left Heschl’s gyrus	3.46
Right middle temporal pole	3.13
Left superior temporal gyrus	3.06
Right middle orbitofrontal cortex	2.91
Left fusiform gyrus	2.83
Right fusiform gyrus	2.28
Left superior occipital gyrus	2.07
Left middle orbitofrontal cortex	2.02
Right superior frontal gyrus	1.99
Left inferior temporal gyrus	1.94

aMCI: Amnesic mild cognitive impairment; NC: normal control.

Pertaining to the classification of NC and AD, negatively contributive brain regions were mainly found in the bilateral temporal lobes and precuneus, while positive regions were located in the bilateral parahippocampal gyrus and orbital frontal lobes (Table 4).

Table 4 | The ten regions that contributed most to the classification of the AD from the NC group

Region	Absolute weight ($\times 10^{-5}$)
Negatively	
Left middle temporal gyrus	4.17
Right supramarginal gyrus	3.76
Left medial orbitofrontal cortex	3.65
Right rectus gyrus	3.6
Right middle temporal gyrus	3.4
Right precuneus	3.26
Right inferior temporal gyrus	3.23
Right inferior parietal gyrus	2.14
Left rectus gyrus	2.14
Left precuneus	2.11
Positively	
Left superior temporal gyrus	3.94
Left parahippocampal gyrus	3.84
Left rolandic operculum	3.59
Right hippocampal gyrus	3.06
Right Heschl gyrus	2.93
Right middle frontal gyrus, orbital part	2.37
Left superior frontal gyrus, orbital part	2.36
Right superior frontal gyrus	2.32
Left Heschl gyrus	2.32
Left amygdala	2.31

AD: Alzheimer’s disease ; NC: normal control.

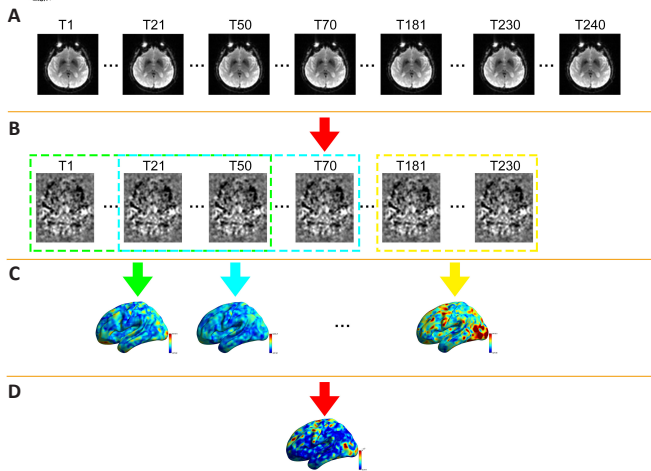


Figure 2 | Process of dFCS calculation.

(A) Raw fMRI. (B) Preprocessed fMRI. (C) Calculation of dFCS atlas using a sliding-window approach. (D) Final atlas of dFCS variance. dFCS: Dynamic functional connectivity strength; fMRI: functional magnetic resonance imaging.



Figure 3 | Five-fold cross validation.

The dataset was divided into five parts for 5-fold cross validation. One part was selected as the test dataset, while the remaining four parts were used as the training dataset. This was repeated five times so that each fold of the data was selected as a test set once, enabling us to obtain the predicted labels for all of the data. 'b' and 'w' in the figure are the parameters of the SVM. Different colored balls represent the samples with different labels.

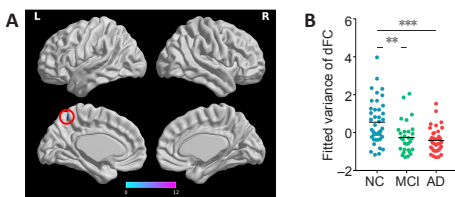


Figure 4 | The difference in dFCS among the NC, aMCI, and AD groups.

(A) The voxel-based analysis revealed a difference in dFCS variance among the NC, aMCI, and AD groups in the left precuneus (red circle). (B) The NC group showed larger dFCS variance in the precuneus than the aMCI and AD groups. Data were analyzed using a two-tailed two-sample *t*-test. $**P < 0.01$; $***P < 0.001$. AD: Alzheimer's disease; aMCI: amnesic mild cognitive impairment; dFCS: dynamic functional connectivity strength; L: left; NC: normal control R: right.

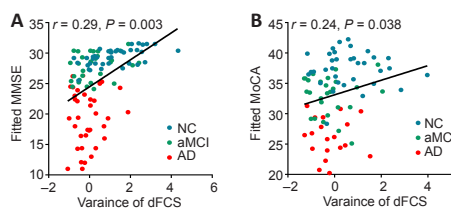


Figure 5 | Correlations between the mean dFCS variance in the precuneus with MMSE (A) and MoCA (B) scores.

Data were analyzed via partial correlation analysis. AD: Alzheimer's disease; aMCI: amnesic mild cognitive impairment; dFCS: dynamic functional connectivity strength; MMSE: Mini-Mental Status Examination; NC: normal control.

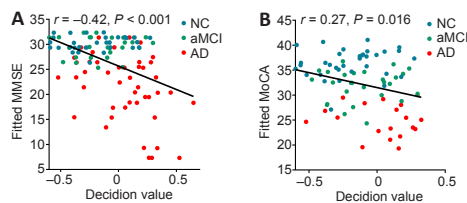


Figure 6 | Correlations between decision value and MMSE (A) and MoCA (B) scores.

Data were analyzed via partial correlation analysis. AD: Alzheimer's disease; aMCI: amnesic mild cognitive impairment; dFCS: dynamic functional connectivity strength; MMSE: Mini-Mental Status Examination; NC: normal control.

Brain networks that most strongly contributed to classification

We also considered the mean positive and negative weights in the brain networks (Yeo et al., 2011). In the aMCI-NC classifier, the DMN and frontoparietal network were the most contributive networks (Figure 7), whereas in the NC-AD classifier, the weights were almost all negative and mainly located in the DMN (Figure 8). For both the aMCI-NC and AD-NC classifiers, the visual network, somatomotor network, ventral attentional network, and limbic network had positive weights, with two clear phenomena. First, the weight of the positive contribution of the above networks was significantly higher in the aMCI-NC group than in the AD group. Second, the contribution weight of the somatomotor network was mainly positive, and its weight was second only to that of the DMN.

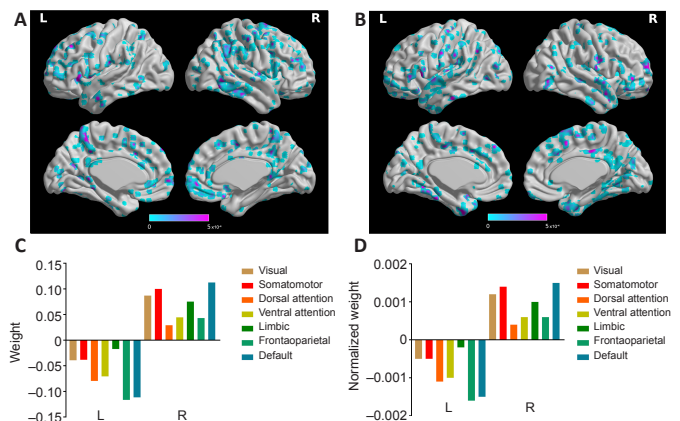


Figure 7 | The weight of classifying the aMCI from the NC group.

(A) The distribution of negative weight. (B) The distribution of positive weight. (C) The weight of different functional networks. (D) The normalized weight (by the volume of the functional network) of different functional weights. "Default" represents the default mode areas. aMCI: Amnesic mild cognitive impairment; L: left; NC: normal control; R: right.

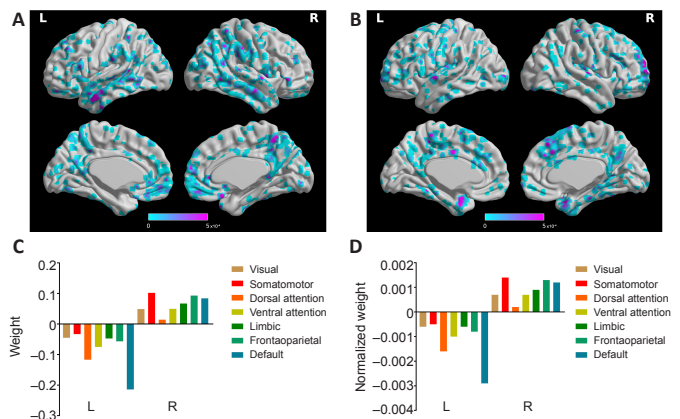


Figure 8 | The weight of classifying the AD from the NC group.

(A) The distribution of negative weight. (B) The distribution of positive weight. (C) The weight of different functional networks. (D) The normalized weight (by the volume of the functional network) of different functional weights. AD: Alzheimer's disease; L: left; NC: normal control; R: right.

Discussion

We found that the dFCS variance in the left precuneus was significantly lower in AD and MCI patients compared with NCs, and that changes in the dFCS variance in the left precuneus were correlated with disease severity. In particular, the partial-correlation analysis showed that changes in dFCS variance in the left precuneus were linked to decreased MMSE scores after controlling for age, sex, and education as confounding variables. In addition, two SVM models were trained to classify AD from NC as well as aMCI from NC. Our results indicated that the AD-NC classifier had better performance than the aMCI-NC classifier. The mean weights across brain regions and brain networks imply that the temporal lobe plays a significant role in the development of AD and MCI, and that the DMN and frontoparietal network play prominent roles in the progression of AD. Together, our results suggest that these neural measures of dynamic connectivity strength may serve as biomarkers that could be used in the diagnosis, treatment, and ongoing assessment of AD.

Altered dFCS variability in the left precuneus in AD patients

Our results indicate that dFCS variance in the left precuneus was significantly reduced in AD and MCI patients compared with healthy older people. The precuneus is the superior parietal part of the medial surface of each cerebral hemisphere, and is located in front of the cuneus (the superior part of the occipital lobe). The precuneus is a main node of the DMN, and part of the precuneus was included in the frontal parietal control network in our study. The precuneus has been associated with various cognitive functions including episodic memory, self-reflection, and other aspects of consciousness (Cavanna and Trimble, 2006). Interestingly, the precuneus shows both functional and structural lateralization. For instance, compared with the right precuneus, the left precuneus was found to exhibit a greater degree of atrophy during normal aging and AD progression (Love and Miners, 2016). Similarly, imaging studies have indicated that the left precuneus is more vulnerable and more susceptible to various neurological disorders, including AD (Fusar-Poli et al., 2011). Furthermore, the functional connectivity of the left precuneus was found to be more vulnerable in AD patients than NCs during memory tasks (Berthoz, 1997). Consistent with the aforementioned findings, we found the most significant dFCS variability in the left precuneus in patients with AD. This dysfunction in the left precuneus may be underpinned by the accumulation of A β and tau proteins in this region in early AD patients (Miners et al., 2016; Baghel et al., 2019). Together, our findings suggest that abnormalities in dFCS variability in the left precuneus have potential as a noninvasive marker for early AD, and that early clinical interventions targeting this region may slow AD or aMCI progression.

In the present study, the mean MMSE score was lowest among AD patients, and we found a positive correlation between mean MMSE score and dFCS variability in the left precuneus after correcting for confounding variables. The MMSE is a rapid and comprehensive measure of overall cognitive function, and is widely used in clinical settings to screen for dementia (Tombaugh and McIntyre, 1992). A series of multicenter validation studies has shown that MMSE scores can accurately describe the trajectory of cognitive change in patients during the course of dementia development (Bergeron et al., 2017). For instance, a previous study found that increased MMSE scores predicted proneness to clinical symptoms in patients with AD (Li et al., 2016). By extending the results of that study, our findings suggest that changes in dFCS variability in the left precuneus might predict declines in cognitive ability during AD progression.

Classification of AD according to changes in brain regions and networks

Previous studies have found that AD patients tend to have altered medial temporal lobe structures, especially hippocampal atrophy, enlarged ventricles, widened capsules, and other signs of brain atrophy. These changes can extend to the frontal lobe, parietal lobe, and cerebellum with disease progression (Villemagne et al., 2018). In the present study, the brain regions that contributed to aMCI and NC classification were mainly distributed in the frontal lobe and temporal lobe, and these brain regions were included in the default network. At the same time, activity in the frontal lobes (including the orbitofrontal cortex), temporal lobes, and occipital lobes in aMCI and AD patients was enhanced compared with that in NCs. Previous studies have also found that MCI patients had excessive activation in the medial temporal lobe region, with reduced functional connectivity between the medial temporal lobe and other brain regions. This indicates that neuronal degeneration

may increase functional connectivity in the medial temporal lobe, which may support performance in some subsystems (Alsop et al., 2010; Pasquini et al., 2015). This region of the orbitofrontal cortex has functional connections with the thalamus, temporal lobe, amygdala, and olfactory system (Aggleton, 2012). In this study, we found different degrees of functional enhancement according to the stage of aMCI and AD. At the onset of AD, multiple brain regions are thought to compensate for neurological changes, thus upholding olfaction, feeding, auditory perception, and the reward system. This suggests that compensatory mechanisms are an indispensable part of the pathophysiological mechanisms of AD. Our brain network-level analysis revealed differences in brain networks between NCs and patients. For the aMCI-NC classifiers, the DMN and frontoparietal network made large cumulative contributions, whereas only the DMN showed a large contribution among the AD-NC classifiers. In addition, compared with the other brain networks, the frontoparietal network made a large contribution in terms of both classifiers, although this was less than the contribution of the DMN.

A series of functional connectivity studies identified that AD and MCI patients are susceptible to changes in the DMN. This is consistent with our findings regarding the prominent contribution of the DMN in both classification models. The DMN is essential for memory, self-related cognitive processes, and cognitive control, which are involved in many cognitive functions in healthy individuals (Greicius et al., 2003). Disrupted DMN activity in AD and MCI patients has been found to contribute to the prominent decline of cognitive abilities. Our study provides new evidence regarding the role of DMN dynamics in distinguishing between AD, MCI, and healthy controls. The DMN plays an important role in self-related processing such as mind-wandering, which is essential for multiple cognitive functions (Vidaurre et al., 2017). Recently, dynamic changes in DMN functional connectivity were significantly implicated in flexible neural computation during both resting-state and cognitive tasks (Jones et al., 2011). Our results extend these findings by suggesting that altered DMN dynamics may contribute to the development of AD by disrupting flexible neural computation.

Our findings regarding abnormalities in dFCS variability in the frontoparietal network in AD and MCI patients are consistent with previous studies. The frontoparietal network is the key component of the triple network structure (Cocchi et al., 2013). It flexibly interacts with the DMN and the salience network to allocate cognitive resources according to task demands in various environments (Cocchi et al., 2013). Altered frontoparietal network connectivity has been associated with disrupted working memory and executive control in many neurodegenerative disease including AD and MCI. For instance, a previous task-based fMRI-based study found that MCI patients exhibited stronger neural activity in the frontal and parietal regions than healthy controls during memory encoding and retrieval, working memory, executive function, and perception-related tasks (Chand et al., 2017). Similarly, a review summarizing 75 fMRI studies reported that MCI patients showed hypoactivation in the frontoparietal cortex relative to healthy controls (Li et al., 2015). Our findings support and extend the conclusions of some studies proposing that AD and MCI share the same neural compensation mechanisms, and therefore, that activity patterns in brain networks should be similar between MCI and AD patients. Furthermore, our results suggest that altered dynamics in the frontoparietal network may be an essential element of AD pathology, which may be related to disrupted flexibility of cognitive control.

In the aMCI-NC classifier, the visual network, somatomotor network, ventral attention network, and edge-centric functional network made large positive contributions to classification. In contrast, in the AD-NC classifier, the positive contribution was relatively low among all networks. This indicates that the brain may enhance the variability of various networks to compensate for cognitive decline in the early stage of aMCI. However, by the late stage of AD, the variability of functional connectivity had decreased, which may signal occurrence of functional compensation. This is consistent with literature indicating that compensation mostly occurs in the MMCI stage, but not in the AD stage (Delli Pizzi et al., 2019; Skouras et al., 2019).

Limitations

This study had several limitations. First, when we calculated dFCS, we summed the values of all voxels rather than the calculated mean value. This may have created a bias towards larger networks because they have more voxels. Second, the results of our analysis suggested that the performance of the classifier in terms of AD diagnosis was

not particularly high, which may have been related to the sample size of the study. However, dFCS is still a good model for studying the pathophysiological mechanisms of AD, and multivariate statistical analysis can serve as a supplement. Our effect size may have been higher if we had used a structural modality. However the goal of our study was to examine this application of functional modalities. Our results may have been limited by the small sample size. Future studies with larger sample sizes are needed.

Considering our relatively small sample size, and our plan to consider the contribution of all of the voxels in terms of dFCS variability in the classification system, we used SVM models because they have computational simplicity and efficiency for small samples (Zendehboudi et al., 2018). However, SVMs have several limitations. For instance, the performance of an SVM decreases when the dimensionality of the features exceeds the number of training data points. The SVM can neither divide the data points on the hyperplane nor describe the points outside the hyperplane in terms of attributes reflecting the distance from the point to the hyperplane. As a result, we could not fully consider the variability of dFCS among the AD patients in this study. Finally, using cross-validation combined with permutation tests, as we did in this study, is the most common solution for small sample problems in almost all machine learning studies. However, the uncertainty of the point estimates obtained using this validation method is unknown, and this uncertainty seems to be greater in biomedical settings (Rodríguez-Pérez et al., 2018). Therefore, future small sample studies should use this method in conjunction with advanced forms such as Bayesian confidence intervals.

Previous studies have shown that AD causes the cerebral cortices, including the temporal, frontal, and parietal lobes, to shrink over time (Chard et al., 2002; Li et al., 2016; Pini et al., 2016). This differs from what we found in the group comparisons. Considering that AD patients in traditional autopsy studies tend to have a more severe disease course than the patients in this study, changes in dFCS in the left precuneus might precede massive gray matter atrophy in other regions such as the temporal lobe. This conjecture should be examined in future longitudinal studies with larger samples. Our classification analysis indicated that the DMN including the temporal lobe contributed to the discrimination of AD patients from healthy controls. This indicates that the temporal lobe in the AD patients in this study may have undergone slight alterations that were not yet sufficient to distinguish between AD patients and healthy controls independently. Together, our findings suggest that clinicians should be concerned about abnormalities in the functional connectivity of the left precuneus. Because of the relatively small sample size in the present study, systematic, large-sample, longitudinal studies focusing on the left precuneus are needed to further validate our results and uncover more details regarding AD pathology.

Conclusion

In this study, we found significant abnormalities in dFCS variability in the left precuneus among AD and MCI patients, which were associated with reduced overall cognitive performance. Furthermore, SVM classification showed that dFCS variability in the DMN and frontoparietal network could be used as significant features to classify AD-HC and MCI-HC. Our findings build upon previous static functional connectivity studies of AD and highlight the important role of dynamics of the precuneus, DMN, and frontoparietal network in flexible computation during the resting-state. Alterations in these neural processes may contribute to the development of AD. Furthermore, our results suggest the potential of dFCS variability, especially in the precuneus, DMN, and frontoparietal network, as an AD imaging marker for the early diagnosis of AD. Considering the relatively small sample size and methodological limitations, the results of this study need to be validated by future research.

Author contributions: Literature retrieval, data analysis and manuscript draft: CZ, WJH; study design: CZ, WJH, XZ, NS; data collection in clinical and neuropsychological tests: CZ, FF, BZ, YEG, LNWX, XZ; data collection in multimodal neuroimaging: HXY, PW; data analysis: WJH, NS; manuscript revision: XZ, NS. All authors approved the final version of this manuscript.

Conflicts of interest: There are no conflicts of interest.

Availability of data and materials: All data generated or analyzed during this study are included in this published article and its supplementary information files.

Open access statement: This is an open access journal, and articles are distributed under the terms of the Creative Commons

AttributionNonCommercial-ShareAlike 4.0 License, which allows others to remix, tweak, and build upon the work non-commercially, as long as appropriate credit is given and the new creations are licensed under the identical terms.

Open peer reviewer: Ian M McDonough, The University of Alabama, USA.

Additional files:

Additional file 1: Hospital ethics approval (Chinese).

Additional file 2: Informed consent form (Chinese).

Additional file 3: STROBE checklist.

Additional file 4: Open peer review report 1.

References

- Aggleton JP (2012) Multiple anatomical systems embedded within the primate medial temporal lobe: implications for hippocampal function. *Neurosci Biobehav Rev* 36:1579-1596.
- Alsop DC, Dai W, Grossman M, Detre JA (2010) Arterial spin labeling blood flow MRI: its role in the early characterization of Alzheimer's disease. *J Alzheimers Dis* 20:871-880.
- Baghel V, Tripathi M, Parida G, Gupta R, Yadav S, Kumar P, Dey AB, Damle NA, Kumar R, Bal C (2019) In vivo assessment of tau deposition in Alzheimer disease and assessing its relationship to regional brain glucose metabolism and cognition. *Clin Nucl Med* 44:e597-e601.
- Bargmann CI, Marder E (2013) From the connectome to brain function. *Nat Methods* 10:483-490.
- Bergeron D, Flynn K, Verret L, Poulin S, Bouchard RW, Bocti C, Fülöp T, Lacombe G, Gauthier S, Nasreddine Z, Laforce RJ (2017) Multicenter validation of an MMSE-MoCA conversion table. *J Am Geriatr Soc* 65:1067-1072.
- Berthoz A (1997) Parietal and hippocampal contribution to topokinetic and topographic memory. *Philos Trans R Soc Lond B Biol Sci* 352:1437-1448.
- Blennow K, Hampel H (2003) CSF markers for incipient Alzheimer's disease. *Lancet Neurol* 2:605-613.
- Buchanan CR, Bastin ME, Ritchie SJ, Liewald DC, Madole JW, Tucker-Drob EM, Deary IJ, Cox SR (2020) The effect of network thresholding and weighting on structural brain networks in the UK Biobank. *Neuroimage* 211:116443.
- Cai Y, Xie M, Su Y, Tong Z, Wu X, Xu W, Li J, Zhao F, Dang C, Chen G, Lan L, Shen J, Zheng Y (2020) Aberrant functional and causal connectivity in acute tinnitus with sensorineural hearing loss. *Front Neurosci* 14:592.
- Cavanna AE, Trimble MR (2006) The precuneus: a review of its functional anatomy and behavioural correlates. *Brain* 129:564-583.
- Chand GB, Wu J, Hajjar I, Qiu D (2017) Interactions of the salience network and its subsystems with the default-mode and the central-executive networks in normal aging and mild cognitive impairment. *Brain Connect* 7:401-412.
- Chard DT, Griffin CM, Parker GJ, Kapoor R, Thompson AJ, Miller DH (2002) Brain atrophy in clinically early relapsing-remitting multiple sclerosis. *Brain* 125:327-337.
- Chaves R, Ramírez J, Górriz JM, López M, Salas-Gonzalez D, Alvarez I, Segovia F (2009) SVM-based computer-aided diagnosis of the Alzheimer's disease using t-test NMSE feature selection with feature correlation weighting. *Neurosci Lett* 461:293-297.
- Chen H, Nomi JS, Uddin LQ, Duan X, Chen H (2017) Intrinsic functional connectivity variance and state-specific under-connectivity in autism. *Hum Brain Mapp* 38:5740-5755.
- Chen J, Sun D, Shi Y, Jin W, Wang Y, Xi Q, Ren C (2018) Alterations of static functional connectivity and dynamic functional connectivity in motor execution regions after stroke. *Neurosci Lett* 686:112-121.
- Cocchi L, Zalesky A, Fornito A, Mattingley JB (2013) Dynamic cooperation and competition between brain systems during cognitive control. *Trends Cogn Sci* 17:493-501.
- Delli Pizzi S, Punzi M, Sensi SL (2019) Functional signature of conversion of patients with mild cognitive impairment. *Neurobiol Aging* 74:21-37.
- Dennis EL, Thompson PM (2014) Functional brain connectivity using fMRI in aging and Alzheimer's disease. *Neuropsychol Rev* 24:49-62.
- Drago V, Babiloni C, Bartrés-Faz D, Caroli A, Bosch B, Hensch T, Didic M, Klafki HW, Pievani M, Jovicich J, Venturi L, Spitzer P, Vecchio F, Schoenkecht P, Wiltfang J, Redolfi A, Forloni G, Blin O, Irving E, Davis C, et al. (2011) Disease tracking markers for Alzheimer's disease at the prodromal (MCI) stage. *J Alzheimers Dis* 26 Suppl 3:159-199.
- Du Y, Pearlson GD, Lin D, Sui J, Chen J, Salman M, Tamminga CA, Ileva EI, Sweeney JA, Keshavan MS, Clementz BA, Bustillo J, Calhoun VD (2017) Identifying dynamic functional connectivity biomarkers using GIG-ICA: Application to schizophrenia, schizoaffective disorder, and psychotic bipolar disorder. *Hum Brain Mapp* 38:2683-2708.
- Duan X, Hu M, Huang X, Su C, Zong X, Dong X, He C, Xiao J, Li H, Tang J, Chen X, Chen H (2020) Effect of risperidone monotherapy on dynamic functional connectivity of insular subdivisions in treatment-naive, first-episode schizophrenia. *Schizophr Bull* 46:650-660.

- Fusar-Poli P, Borgwardt S, Crescini A, Deste G, Kempton MJ, Lawrie S, Mc Guire P, Sacchetti E (2011) Neuroanatomy of vulnerability to psychosis: a voxel-based meta-analysis. *Neurosci Biobehav Rev* 35:1175-1185.
- Grady CL, Haxby JV, Horwitz B, Sundaram M, Berg G, Schapiro M, Friedland RP, Rapoport SI (1988) Longitudinal study of the early neuropsychological and cerebral metabolic changes in dementia of the Alzheimer type. *J Clin Exp Neuropsychol* 10:576-596.
- Greicius MD, Krasnow B, Reiss AL, Menon V (2003) Functional connectivity in the resting brain: a network analysis of the default mode hypothesis. *Proc Natl Acad Sci U S A* 100:253-258.
- Haller S, Lovblad KO, Giannakopoulos P (2011) Principles of classification analyses in mild cognitive impairment (MCI) and Alzheimer disease. *J Alzheimers Dis* 26 Suppl 3:389-394.
- Huang Y, Xu L, Kuang L, Wang W, Cao J, Xiao MN (2020) Abnormal brain activity in adolescents with Internet addiction who attempt suicide: an assessment using functional magnetic resonance imaging. *Neural Regen Res* 15:1554-1559.
- Hutchison RM, Womelsdorf T, Allen EA, Bandettini PA, Calhoun VD, Corbetta M, Della Penna S, Duyn JH, Glover GH, Gonzalez-Castillo J, Handwerker DA, Keilholz S, Kiviniemi V, Leopold DA, de Pasquale F, Sporns O, Walter M, Chang C (2013) Dynamic functional connectivity: promise, issues, and interpretations. *Neuroimage* 80:360-378.
- Jack CR, Jr., Wiste HJ, Vemuri P, Weigand SD, Senjem ML, Zeng G, Bernstein MA, Gunter JL, Pankratz VS, Aisen PS, Weiner MW, Petersen RC, Shaw LM, Trojanowski JQ, Knopman DS (2010) Brain beta-amyloid measures and magnetic resonance imaging atrophy both predict time-to-progression from mild cognitive impairment to Alzheimer's disease. *Brain* 133:3336-3348.
- Jones DT, Machulda MM, Vemuri P, McDade EM, Zeng G, Senjem ML, Gunter JL, Przybelski SA, Avula RT, Knopman DS, Boeve BF, Petersen RC, Jack CR, Jr. (2011) Age-related changes in the default mode network are more advanced in Alzheimer disease. *Neurology* 77:1524-1531.
- Li H, Jia J, Yang Z (2016) Mini-Mental State Examination in elderly Chinese: a population-based normative study. *J Alzheimers Dis* 53:487-496.
- Li HJ, Hou XH, Liu HH, Yue CL, He Y, Zuo XN (2015) Toward systems neuroscience in mild cognitive impairment and Alzheimer's disease: a meta-analysis of 75 fMRI studies. *Hum Brain Mapp* 36:1217-1232.
- Liao W, Li J, Duan X, Cui Q, Chen H, Chen H (2018) Static and dynamic connectomics differentiate between depressed patients with and without suicidal ideation. *Hum Brain Mapp* 39:4105-4118.
- Logothetis NK, Wandell BA (2004) Interpreting the BOLD signal. *Annu Rev Physiol* 66:735-769.
- Love S, Miners JS (2016) Cerebrovascular disease in ageing and Alzheimer's disease. *Acta Neuropathol* 131:645-658.
- Luo Y, He H, Duan M, Huang H, Hu Z, Wang H, Yao G, Yao D, Li J, Luo C (2019) Dynamic functional connectivity strength within different frequency-band in schizophrenia. *Front Psychiatry* 10:995.
- Lv W, Xue Y (2010) Prediction of acetylcholinesterase inhibitors and characterization of correlative molecular descriptors by machine learning methods. *Eur J Med Chem* 45:1167-1172.
- Ma X, Wu D, Mai Y, Xu G, Tian J, Jiang G (2020) Functional connectome fingerprint of sleep quality in insomnia patients: Individualized out-of-sample prediction using machine learning. *Neuroimage Clin* 28:102439.
- McDade E, Bateman RJ (2017) Stop Alzheimer's before it starts. *Nature* 547:153-155.
- McKhann G, Drachman D, Folstein M, Katzman R, Price D, Stadlan EM (1984) Clinical diagnosis of Alzheimer's disease: report of the NINCDS-ADRDA Work Group under the auspices of Department of Health and Human Services Task Force on Alzheimer's Disease. *Neurology* 34:939-944.
- Miners JS, Palmer JC, Love S (2016) Pathophysiology of hypoperfusion of the precuneus in early Alzheimer's disease. *Brain Pathol* 26:533-541.
- Pantoni L, Inzitari D (1993) Hachinski's ischemic score and the diagnosis of vascular dementia: a review. *Ital J Neurol Sci* 14:539-546.
- Pasquini L, Scherr M, Tahmasian M, Meng C, Myers NE, Ortner M, Mühlau M, Kurz A, Förstl H, Zimmer C, Grimmer T, Wohlschläger AM, Riedl V, Sorg C (2015) Link between hippocampus' raised local and eased global intrinsic connectivity in AD. *Alzheimers Dement* 11:475-484.
- Pereira F, Mitchell T, Botvinick M (2009) Machine learning classifiers and fMRI: a tutorial overview. *Neuroimage* 45:199-209.
- Petersen RC (2004) Mild cognitive impairment as a diagnostic entity. *J Intern Med* 256:183-194.
- Petersen RC, Caracciolo B, Brayne C, Gauthier S, Jelic V, Fratiglioni L (2014) Mild cognitive impairment: a concept in evolution. *J Intern Med* 275:214-228.
- Petersen RC, Doody R, Kurz A, Mohs RC, Morris JC, Rabins PV, Ritchie K, Rosser M, Thal L, Winblad B (2001) Current concepts in mild cognitive impairment. *Arch Neurol* 58:1985-1992.
- Pini L, Pievani M, Bocchetta M, Altomare D, Bosco P, Cavedo E, Galluzzi S, Marizzoni M, Frisoni GB (2016) Brain atrophy in Alzheimer's disease and aging. *Ageing Res Rev* 30:25-48.
- Rashid B, Damaraju E, Pearlson GD, Calhoun VD (2014) Dynamic connectivity states estimated from resting fMRI Identify differences among Schizophrenia, bipolar disorder, and healthy control subjects. *Front Hum Neurosci* 8:897.
- Rashid B, Arbabshirani MR, Damaraju E, Cetin MS, Miller R, Pearlson GD, Calhoun VD (2016) Classification of schizophrenia and bipolar patients using static and dynamic resting-state fMRI brain connectivity. *Neuroimage* 134:645-657.
- Rodríguez-Pérez R, Fernández L, Marco S (2018) Overoptimism in cross-validation when using partial least squares-discriminant analysis for omics data: a systematic study. *Anal Bioanal Chem* 410:5981-5992.
- Schultz AP, Chhatwal JP, Hedden T, Mormino EC, Hanseeuw BJ, Sepulcre J, Huijbers W, LaPoint M, Buckley RF, Johnson KA, Sperling RA (2017) Phases of hyperconnectivity and hypoconnectivity in the default mode and salience networks track with amyloid and tau in clinically normal individuals. *J Neurosci* 37:4323-4331.
- Skouras S, Falcon C, Tucholka A, Rami L, Sanchez-Valle R, Lladó A, Gispert JD, Molinuevo JL (2019) Mechanisms of functional compensation, delineated by eigenvector centrality mapping, across the pathophysiological continuum of Alzheimer's disease. *Neuroimage Clin* 22:101777.
- Smith SM, Nichols TE (2009) Threshold-free cluster enhancement: addressing problems of smoothing, threshold dependence and localisation in cluster inference. *Neuroimage* 44:83-98.
- Sperling RA, Aisen PS, Beckett LA, Bennett DA, Craft S, Fagan AM, Iwatsubo T, Jack CR, Jr., Kaye J, Montine TJ, Park DC, Reiman EM, Rowe CC, Siemers E, Stern Y, Yaffe K, Carrillo MC, Thies B, Morrison-Bogorad M, Wagster MV, et al. (2011) Toward defining the preclinical stages of Alzheimer's disease: recommendations from the National Institute on Aging-Alzheimer's Association workgroups on diagnostic guidelines for Alzheimer's disease. *Alzheimers Dement* 7:280-292.
- Suzuki H, Venkataraman AV, Bai W, Guillon F, Guo Y, Dehghan A, Matthews PM (2019) Associations of regional brain structural differences with aging, modifiable risk factors for dementia, and cognitive performance. *JAMA Netw Open* 2:e1917257.
- Tiwari S, Atluri V, Kaushik A, Yndart A, Nair M (2019) Alzheimer's disease: pathogenesis, diagnostics, and therapeutics. *Int J Nanomedicine* 14:5541-5554.
- Tombaugh TN, McIntyre NJ (1992) The mini-mental state examination: a comprehensive review. *J Am Geriatr Soc* 40:922-935.
- Tzourio-Mazoyer N, Landeau B, Papathanassiou D, Crivello F, Etard O, Delcroix N, Mazoyer B, Joliot M (2002) Automated anatomical labeling of activations in SPM using a macroscopic anatomical parcellation of the MNI MRI single-subject brain. *Neuroimage* 15:273-289.
- Vidaurre D, Smith SM, Woolrich MW (2017) Brain network dynamics are hierarchically organized in time. *Proc Natl Acad Sci U S A* 114:12827-12832.
- Villemagne VL, Doré V, Burnham SC, Masters CL, Rowe CC (2018) Imaging tau and amyloid- β proteinopathies in Alzheimer disease and other conditions. *Nat Rev Neurol* 14:225-236.
- von Elm E, Altman DG, Egger M, Pocock SJ, Gtzsche PC, Vandenbroucke JP; STROBE Initiative (2007) The Strengthening of Reporting of Observational Studies in Epidemiology (STROBE) statement: guidelines for reporting observational studies. *PLoS Med* 4:e296.
- Wang Q, He C, Wang Z, Zhang Z, Xie C (2021) Dynamic connectivity alteration facilitates cognitive decline in Alzheimer's disease spectrum. *Brain Connect* 11:213-224.
- Wenk GL (2003) Neuropathologic changes in Alzheimer's disease. *J Clin Psychiatry* 64 Suppl 9:7-10.
- Xing XX, Zheng MX, Hua XY, Ma SJ, Ma ZZ, Xu JG (2021) Brain plasticity after peripheral nerve injury treatment with massage therapy based on resting-state functional magnetic resonance imaging. *Neural Regen Res* 16:388-393.
- Yang S, Meng Y, Li J, Fan YS, Du L, Chen H, Liao W (2019) Temporal dynamic changes of intrinsic brain activity in schizophrenia with cigarette smoking. *Schizophr Res* 210:66-72.
- Yeo BT, Krienen FM, Sepulcre J, Sabuncu MR, Lashkari D, Hollinshead M, Roffman JL, Smoller JW, Zöllei L, Polimeni JR, Fischl B, Liu H, Buckner RL (2011) The organization of the human cerebral cortex estimated by intrinsic functional connectivity. *J Neurophysiol* 106:1125-1165.
- Zendehboudi A, Baseer MA, Saidur R (2018) Application of support vector machine models for forecasting solar and wind energy resources: A review. *J Clean Prod* 199:272-285.
- Zeng Q, Luo X, Li K, Wang S, Zhang R, Hong H, Huang P, Jiaerken Y, Xu X, Xu J, Wang C, Zhou J, Zhang M (2019) Distinct spontaneous brain activity patterns in different biologically-defined Alzheimer's disease cognitive stage: a preliminary study. *Front Aging Neurosci* 11:350.
- Zhao T, Wang D, Hu Y, Zhang N, Zang T, Wang Y (2019) Identifying Alzheimer's disease-related miRNA based on semi-clustering. *Curr Gene Ther* 19:216-223.
- Zou QH, Zhu CZ, Yang Y, Zuo XN, Long XY, Cao QJ, Wang YF, Zang YF (2008) An improved approach to detection of amplitude of low-frequency fluctuation (ALFF) for resting-state fMRI: fractional ALFF. *J Neurosci Methods* 172:137-141.

P-Reviewer: McDonough IM; C-Editor: Zhao M; S-Editors: Yu J, Li CH; L-Editors: Yu J, Song LP; T-Editor: Jia Y